Journal of Energy Storage 86 (2024) 111306

Contents lists available at ScienceDirect

Journal of Energy Storage

journal homepage: www.elsevier.com/locate/est

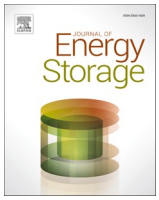

Research Papers

Optimal scheduling of a microgrid based on renewable resources and demand response program using stochastic and IGDT-based approach

Sahar Seyedeh-Barhagh [a,b], Mehdi Abapour [a], Behnam Mohammadi-Ivatloo [a,c], Miadreza Shafie-Khah [b], Hannu Laaksonen [b,*]

[a] Faculty of Electrical and Computer Engineering, University of Tabriz, Tabriz, Iran
[b] School of Technology and Innovations University of Vaasa, Vaasa, Finland
[c] Department of Electrical Engineering, School of Energy Systems, LUT University, Finland

ARTICLE INFO

Keywords:
Optimal operation
Renewable generation
Microgrid
Demand response
Uncertainty management
Photovoltaic system
Electric vehicle

ABSTRACT

Optimal economic scheduling of microgrids with photovoltaic (PV) and wind generation has gained increased attention during recent years. Integration of renewable energy resources in microgrids requires increasingly active control and management of energy storages and demand response (DR). In this paper, a risk-based stochastic optimal energy management model is developed for microgrid with renewables, energy storage and load control by time-of-use-based DR programs. Microgrid includes PV system, wind system, micro-turbine, fuel cell, electric vehicle (EV), and energy storage. Information-gap decision theory (IGDT) is employed to address the uncertainty of loads and to provide the operating strategies for the microgrid controllable energy resources. This proposed model has been solved as a mixed-integer non-linear programming (MINLP) in General Algebraic Modeling System (GAMS) software and simulation results in different conditions are studied and discussed. Three different risk management strategies have been studied such as risk-averse, risk-neutral and risk-seeker mode. The simulation results indicate that the impacts of risk-averseness or risk-seeker of the decision maker affect the system operation. For instance, the results showed the DR program's role in risk-averse and risk-taking strategies, impacting consumption and costs. The proposed model ensures the risk-averse decision-maker that if the uncertain parameter deviates within the optimum robustness region, the final cost will not exceed the critical cost. On the other hand, the risk-seeking decision-maker can reach lower final costs by accepting the risks if the uncertain parameter deviates favorably within the opportunity region. Decision-makers can manage risks by adjusting consumption. Thus, considering the cost of risk management is crucial, as it increases with robust or opportunistic approaches.

1. Introduction

In recent years, the world has been grappling with the challenge of diminishing fossil fuel reserves. To address this pressing issue, there has been a growing trend towards distributed energy resources and electric vehicles as viable alternatives. These two solutions have emerged as crucial components of the global response, offering a multitude of benefits and complementing each other in various ways. Distributed energy resources, such as solar panels, wind turbines, and microgrids, have gained significant attention due to their decentralized nature. Unlike traditional energy sources that rely on centralized power plants, distributed energy resources empower individuals, communities, and businesses to generate their own clean and renewable energy. This decentralized approach not only reduces dependence on fossil fuels but also enhances energy resilience and security, allowing for a more sustainable and self-sufficient energy ecosystem. Electric vehicles (EVs), on the other hand, have rapidly emerged as a game-changer in the transportation sector. With zero tailpipe emissions, EVs offer a cleaner and greener alternative to conventional internal combustion engine vehicles. They contribute to mitigating air pollution, reducing greenhouse gas emissions, and combating climate change. Additionally, EVs also present opportunities for integrating with the electricity grid through vehicle-to-grid (V2G) technology, enabling bidirectional energy flow and grid stabilization. This synergy between EVs and distributed energy resources paves the way for a more efficient and flexible energy system. Furthermore, the features of distributed energy resources and electric vehicles make them highly compatible and mutually reinforcing. The

* Corresponding author.
E-mail address: hannu.laaksonen@uwasa.fi (H. Laaksonen).

https://doi.org/10.1016/j.est.2024.111306
Received 2 November 2023; Received in revised form 21 February 2024; Accepted 10 March 2024
Available online 25 March 2024

Nomenclature

$Cost^{Total}$	The total operation cost of microgrid (€)
$Cost^{DER}$	the total cost of distributed generation resources (€)
$Cost^{ESS}$	the total operation cost of storage (€)
$Cost^{GRID}$	the total cost of power exchange with the upstream grid (€)
$Cost^{IMP}$	the amount of total cost related to the imported amount of power from the grid (€)
Rev^{EXP}	the amount of obtained profit from the exported amount of power to the grid (kW)
$P_{t,s}^{PVrooftop}$	is the output power of the PV system in each scenario (kW)
$P_{t,s}^{WINDout}$	the output power of the wind turbine (kW)
P_t^{FU}	the output power of the fuel cell (kW)
P_t^{MT}	the output power of the micro turbine (kW)
$P_{t.dis}^{ESS}$	the discharge power of storage (kW)
$P_{t,s}^{IMP}$	the imported amount of power from the grid (kW)
$P_{t,s}^{EXP}$	The exported power to the grid (kW)
$P_t^{l.DRP}$	the amount of load with regarding demand response program (kW)
P_t^{chev}	the charging power of EV(kW)
P_t^{dchev}	the discharging power of EV (kW)
P_{stc}^{pv}	output of the power of the PV system at the standard condition and the maximum power point (kW)
$T_{t,s}^{c}$	temperature of cells in the PV system
SOC_t	the SOC of EV (kWh)
SOC_t^{Arive}	the SOC of EV upon the arrival time (kWh)
the maximum correlated value.	
λ^{PV}	the operation cost of the PV system (€ct/kWh)
λ^{WIND}	the operation cost of the wind turbine (€ct/kWh)
λ^{FU}	the operation cost of the fuel cell (€ct/kWh)
λ^{MT}	the operation cost of micro turbine (€ct/kWh)
SUC^{MT}	the cost of turning on the microturbine (€)
SDC^{MT}	the cost of turning off the microturbine (€)
SUC^{FU}	the cost of turning on the fuel cell (€)
SDC^{FU}	the cost of turning off the fuel cell (€)
λ^{ESS}	the operation cost of the ESS (€ct/kWh)
λ_t^{IMP}	the imported power price (€ct/kWh)
λ_t^{EXP}	the exported power price (€ct/kWh)
P_{Min}^{IMP}	the minimum imported power from the grid (kW)
P_{Max}^{IMP}	the maximum imported power from the grid (kW)
P_{Min}^{EXP}	the minimum exported power from the grid (kW)
P_{Max}^{EXP}	the maximum exported power from the grid (kW)
P_{Min}^{MT}	the minimum limitations of micro turbine (kW)
P_{Max}^{MT}	The maximum limitations of micro turbine (kW)
P_{Min}^{FU}	The minimum limitation power of fuel cell (kW)
P_{Max}^{FU}	the maximum limitation power of fuel cell (kW)
P_t^{ESS}	the capacity of the ESS
η_{ch}	The charging rates of ESS %
η_{dis}	The discharging rates of ESS %
P_{Min}^{ESS}	The minimum capacity of ESS (kW)
P_{Max}^{ESS}	The maximum capacity of ESS (kW)
n_{se}^{pv}	shows the PV panel numbers that are installed in series
n_{pa}^{pv}	indicates the PV panel numbers that are installed in parallel
$I_{d,s}$	The direct normal irradiance
θ_{φ}	the incidence angle of solar radiation on a tilted surface are modeled
$I_{dif,s}$	diffuse horizontal irradiance
φ	the tilted angle
ρ	the surrounding reflection
$I_{g,s}$	the global horizontal irradiance
ψ	the coefficient related to the PV system's temperature
$T_{t,s}^{a}$	the ambient nominal temperatures (°C)
NCT	the cell nominal temperatures (°C)
η_t^{chev}	The charging ratios of EV %
η_t^{dchev}	The discharging ratios of EV %
SOC_{Max}^{Arive}	the maximum correlated value (kWh)
SOC_t^{Dep}	the SOC of EV upon departure SOC of EV upon departure (kWh)
$SOC_{desired}^{Dep}$	the SOC of EV upon desired SOC of EV upon departure (kWh)

intermittent nature of renewable energy generation can be complemented by the ability of EVs to store and discharge electricity, effectively acting as mobile energy storage devices. This enables EVs to serve as a flexible energy resource, providing grid services, balancing supply and demand, and supporting the integration of renewable energy sources into the grid. Moreover, the expanding charging infrastructure for EVs can also leverage the excess electricity generated by distributed energy resources, maximizing their utilization and further promoting sustainable energy practices. Distributed generation (DG) units can play a significant role in the modern energy systems. On the other hand the increased penetration of electric vehicles has gained attention in recent years. Potentially controlled charging of EVs can provide different flexibility services in power systems for transmission and distribution system operator needs. Electric vehicles together with other energy resources have been studied from different perspectives in literature. For example, in [1] an improved method was presented for a smart parking lot with hydrogen storage system (HSS). This model consisted of an electrolyzer, a hydrogen storage tank, and fuel cell as well as load demand considering technical and economic constraints. On the other hand, by implementing the population-based technique and particle swarm optimization (PSO) algorithm, the cost of operation in the distribution system could be minimized. With the aim of optimally managing the energy of intelligent parking lot containing local dispatchable generators and renewable resources, demand response programming has been used in [2]. According to this study, the load curve was flattened and the operation cost of charging and discharging intelligent parking lot, cost of the upstream grid and local dispatchable generators have been minimized. In [3], an intelligent parking lot -based on solar photovoltaic, was studied. In this model, the economic and environmental performances of the parking lot have been boosted, and the total emission and operation cost of intelligent parking have been decreased. It is worth to mention that fuzzy decision making and weighted sum algorithms have been utilized for solving such a problem with multiple objective functions. Authors in [4] have proposed an optimization model based on genetic algorithm which maximizes the solar energy generation. Besides that, the electric vehicles with various charging methods were harmonized by solar resources in [4]. A bi-objective optimization model has been proposed for better environmental performance and economical operation of the intelligent parking lot in [5], where the impact of time-of-use (TOU) rates of demand response program has been assessed. In [6], a comprehensive review about using solar system in electric vehicle's parking lots has been presented. In the mentioned study, environmental, technical, and financial aspects of electric vehicle parking lots have been studied and

discussed.

Many reviews and previous research have been made related to modeling of EV charging and PV power production. However, there still exists lack of knowledge about the opportunities of their combined modeling. For instance, in [7], PV power production ramp-rate modeling besides quantifying the aggregate clear-sky index on city-scale have been considered accurately in order to fill these research gaps. Electric power capacity of EV parking lot with PV sunshade novel mathematic models have been presented in [8], where the efficiency of battery charger on the amount of demand during charging time has been studied. In [9], a two-stage stochastic model for day-ahead risk constrained scheduling of components in a multi-energy microgrid has been suggested. These components include renewable resources, charging stations for EVs and hydrogen vehicles, combined heat and power (CHP), hydrogen electrolyzers, boilers, cryptocurrency miners, electrical storage system, thermal storage system, HSS, DR programs, and pool markets. Demand uncertainty, EVCS and HVCS, CM, PV and wind generation, as well as the cost of electricity purchased from the pool market, have all been considered. The proposed model's goal was to reduce expected operation costs. A proposed operation strategy for the solar-powered EV parking lots has been provided in [10]. The model maximizes the benefits while also taking the comfort of the EV owner into consideration when the EV parking lots participate in several energy and ancillary service marketplaces, including the implications of capacity fees. Numerous factors, including weather patterns and EV owners' unpredictable schedules, are taken into account in the suggested concept and design.

For Parking Lot Aggregators (PLA), [11] presented a multi-stage stochastic-based structure to integrate plug-in electrical vehicle (PEV) flexibility into the power system. The suggested method traded the PEVs' flexibility in the short-term electricity market on three trading stages, including the day-ahead, adjustment, and balancing markets, from 24 h prior to the energy delivery time until almost real-time. A data-driven strategy was developed to extract PEV behavior in Shopping Center Parking Lots. There was an obvious requirement for near real-time optimization, and the recommended data-driven strategy made it possible to optimize the charging/discharging operation of a large number of PEVs with low time and computational loads. By trading integrated flexibility across three levels of the energy market, the PLA increased market players' profits rather than providing subsidies for responsive PEV owners. The suggested strategy gave electricity markets functional flexibility in addition to maximizing the income of PEV owners. [12] concentrated on the optimal operation of power, heat, and hydrogen-based microgrid combined with solar energy and PEV to reduce daily costs taking heating, electrical loads, and industrial hydrogen application into account. In order to increase the system's flexibility, PEV was considered in the integrated scheduling of power, heat, and hydrogen-based microgrid. Additionally, the risk of random parameters was managed, and the uncertainty of the predicted cost reduced, using the risk assessment based on the conditional value-at-risk (CVaR) criterion.

The authors in [13] developed a stochastic-interval model for scheduling photovoltaic-assisted charging stations, incorporating solar generation and energy price uncertainties. The model solved mixed-integer linear programming and quadratic programming problems and was validated through a benchmark case study. In [14] multiple electricity-hydrogen integrated charging stations (EHI-CSs) were considered as a single entity, managed by an aggregator through controllable facilities and adjustment methods. A two-stage energy management system (EMS) coordinated day-ahead scheduling and real-time dispatch, optimizing costs for the EHI-CSs unit.

A finite-horizon Markov decision process model for optimal management of PV-assisted EV charging stations was developed in [15]. The model utilized vehicle-to-grid (V2G) technology, accounting for fluctuating power prices and unpredictable parking habits. It employed a modified bounded real-time dynamic programming algorithm for computational efficiency. [16] introduced an operation approach for a grid-connected microgrid with high RES and EV integration. It employed a two-stage strategy based on day-ahead and real-time energy markets. A multi-layer energy management system guided the microgrid, considering operational expenses, network constraints, distributed generations, energy storage systems, and EV parking capacities. Uncertainties in load, renewable power, energy prices, and EV parameters were addressed using stochastic programming. This approach combined Monte Carlo simulation with a fast backward/forward method, allowing for effective modeling of these uncertainties.

In [17], presented a flexible multi-objective optimization methodology for vehicle-to-grid and grid-to-vehicle technologies. It considered techno-economic and environmental factors, including PEV battery life cycle, charging/discharging patterns, and driving behaviors. Simulations on an IEEE 69-bus test system aimed to minimize operating costs and CO2 emissions using the Firefly algorithm within a stochastic optimization framework. Furthermore, a probabilistic energy capacity model of EV parking lot has presented in [18], the sequential Monte-Carlo simulations has been used to determine the available storage capacity of a sample parking lot. In order to model the diverse uncertainties such as the plug-in hybrid electric vehicles, the amount of available energy in the battery upon the arrival time, a real-time energy management algorithm has been utilized to minimize the overall daily cost of charging the plug-in hybrid electric vehicles and impact of charging park on the main grid in [19]. For determining the adoptive price of charging and discharging prices in [20], a cooperative game model has been employed to maximize the utilities' profit, and minimize the parking lots cost. Electric vehicles, supported with solar system, have been optimally scheduled in [21]. By using the solar system, the imported power from the grid during the high peak pricing period has been minimized thus, the profit of the parking lot owner has been increased.

The authors in [22] proposed a model to find the optimum size of the renewable energy resources, i.e. PV and energy storage unit in the charging system of the EVs. They solve this problem using the PSO approach. The objective function of this model includes the grid tariff, EV demand and buying/selling prices of the renewable energy resources. A taxonomy table is provided to compare some of the recent similar models with the current proposed microgrid in Table 1. It can be seen that all of these papers offer approaches to integrating RESs and EVs into power systems, but they also exhibit certain limitations that our proposed model addresses. The authors in [1] and [2] consider vehicle-to-grid technologies and DERs like PV and wind, but they do not fully account for uncertainties in load and other RESs. The authors in [3] includes wind as a DER and also have EVs, but it overlooks PV and demand response programs. Meanwhile, [4] focuses solely on cost reduction, without considering any DERs or uncertainties in load. Regarding the uncertainty consideration, the authors in [5] take into account uncertainties in load and includes ESS and RESs, but they do not consider PV, wind, DRP, and EVs. On the other hand, our proposed model takes a comprehensive approach by considering a wide range of energy sources and uncertainties. It includes uncertainties in load, PV, and wind as DERs, which provides a more holistic view of the power system. In addition, it includes DRP, EVs, and ESS to main objective of maximizing/minimizing the horizon of the uncertainty in the robustness/opportunity region towards optimizing the microgrid operation.

This paper develops an optimization framework for risk-based integration of distributed generation units and DR into operation of microgrids under and stochastic environment. In order to model the uncertainties and renewable units and load in microgrid, scenario-based method and information gap decision theory are implemented. The proposed model would benefit from the flexibility of energy resources like EV and DR to result in the least operation cost for the operation of microgrid under the mentioned uncertainties.

The main contributions of this model are listed in bullets as follows:

Table 1
A comparison of the similar models with the proposed approach.

No.	Uncertainty				DRP	EV	ESS	DERs				Objective function
	Load	PV	Wind	EV				RESs		μ-turbine	fuel cell	
								PV	wind			
[23]	✓	✓	✓	✓	×	✓	×	✓	✓	✓	✓	Minimize two objective functions including the operating costs and CO2 emissions
[24]	×	×	✓	✓	✓	✓	✓	×	✓	×	×	Reduce generation costs and emissions
[25]	–	×	–	✓	×	✓	×	✓	×	×	×	Reduce the total costs
[26]	×	×	×	×	×	✓	✓	✓	✓	×	✓	Reduce the cost
[27]	✓	✓	✓	×	×	✓	✓	✓	×	×	×	Maximizing profit
[28]	×	×	×	–	×	✓	×	✓	✓	×	×	Adjust the energy consumption in three market floors
[29]	×	×	–	✓	×	✓	×	✓	×	×	×	Maximize profits
[30]	✓	✓	✓	✓	✓	✓	✓	✓	✓	×	✓	Minimizing expected operation cost
Model	✓	✓	✓	✓	✓	✓	✓	✓	✓	✓	✓	Maximizing the robustness region/Minimizing the opportunity region

- Innovative Optimization Framework: This model presents an optimization framework for risk-based integration of DERs and DR into the operation of microgrids. This approach ensures a more reliable and efficient operation of microgrids, even under a stochastic environment.
- Advanced Methodologies for Uncertainty Modeling: The model employs a scenario-based method and information gap decision theory to effectively handle the uncertainties associated with renewable units and load in the microgrid that can be useful for the decision-makers with complete and incomplete information.
- Leveraging Flexibility of Energy Resources: The proposed model optimizes the use of flexible energy resources like electric vehicles and demand response. This results in the least operation cost for the operation of the microgrid under the mentioned uncertainties, leading to significant cost savings and efficient operation of microgrids.

2. Information-gap approach

In the information-gap approach, the main objective is to maximize the uncertainty horizon the horizon of the uncertainty, while guaranteeing reaching to a certain amount of the expected objective value. In this model, a series of the uncertain parameters are considered to be known by the decision maker. Thus, the optimization process will find a solution that at least the predetermined expected profit is achieved. Three components are required in the information-gap approaches are explained briefly, as follows [31]:

1) System Model: In the IGDT method, there is an input/output system denoted as $R(q,u)$ which is called as the system model. The system model represents the amount of profit of the decision maker. In $R(q, u)$, q is used to indicate the decision variable and u is employed to represent the uncertain parameter. Hence, the system model in the information-gap approach is a function that is dependent to the decision variable and the uncertain parameter. $R(q,u)$ in our work is the operation cost of the microgrid.

2) Uncertainty Model: Characterization of the uncertainty model, denoted as $U(\alpha,\tilde{u})$, in the information-gap approach can be done through various models. Various uncertainty models used in IGDT based programs are named and explained in detail in [32]. We are using one of the most common uncertainty models in our problem formulation that is named fractional uncertainty model, which its mathematical representation is written down below:

$$U(\alpha,\tilde{u}) = \left\{u : \left|\frac{u-\tilde{u}}{\tilde{u}}\right| \le \alpha\right\}, \alpha \ge 0 \quad (1)$$

According to Eq. (1), $U(\alpha,\tilde{u})$ shows the gap that is between the uncertain parameter, i.e. u, and the forecasted or expected amount of the correlated uncertain parameter, i.e. $\tilde{u}$. It is important to note that $\tilde{u}$ is known by the decision maker. α indicates the horizon of the uncertainty. As the horizon of the uncertain parameter increases, greater ranges for the α is expected. It should be noted that the uncertainty model in the info-gap approach has the Contraction and Nesting nature [33]. The second important note about the uncertainty model is that due to the variable characteristic of α, the upper and lower bound of the horizon of the uncertainty will be found by the solver. In other words, the length of the uncertainty horizon is indicated by the amount of the uncertainty parameter. Fig. 1 tries to clarify the uncertainty horizon using the IGDT method. It can be seen that the decision-maker is trying to extend the uncertainty horizons of as much as possible while the observed cost does not exceed the critical cost.

3) Performance Requirement: Various performance models can be specified within the info-gap approach based on the strategy that the decision maker considers for the risk management. In this context, we have considered robustness function as the performance model because of its capability to specify the worst-case scenarios. For the risk-averse decision makers, implementation of the robustness function as the performance model in IGDT approach is a proper option. This performance model operates in a way that to make the decision maker immune against the deviations of the uncertain parameter that are not favorable. In this work, performance model is denoted by $\tilde{\alpha}(q, rc)\tilde{\alpha}(q, rc)$, which its definition is explained as follows: The maximum amount of the uncertain parameter, i.e. $\alpha\alpha$, while fulfilling the minimum requirement of the expected cost of the microgrid in the favorable way:

$$\overline{\alpha}(q, r_c) = max_{\alpha}\{\alpha : \{minimum\ requirment\ r_c\ is\ always\ fulfilled\}\} \quad (2)$$

where r_c is considered as the critical profit of the performance model which is assumed to be at least equal or even better than the expected amount.

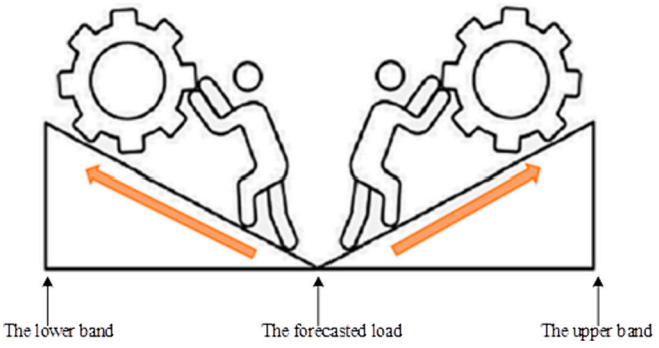

Fig. 1. Illustrating a simple fractional uncertainty model for robustness IGDT method.

3. Problem formulation

The components of the studied microgrid system are shown in Fig. 2 including electrical energy storage unit, combined EV and PV unit, a fuel cell unit, a micro-turbine and wind generator. The energy flow of the electrical energy storage is bidirectional and it means that it can be charged through the microgrid components including the distributed generation units, renewable energy resources and also upstream grid. Moreover, it can be discharged to cover a certain percentage of the load, approximately 30 %. The objective of this proposed model is to minimize the total costs of the studied microgrid.

The objective function of the studied problem, presented in Eqs. (3)–(9), is to minimize the operating cost of the microgrid including solar system, EV, wind, microturbine, fuel cell and storage.

$$Min\ obj = Cost^{Total} = Cost^{DER} + Cost^{ESS} + Cost^{GRID} \tag{3}$$

where, *obj* is the objective function, $Cost^{Total}$ is the total operation cost of microgrid, $Cost^{DER}$ is the total cost of distributed generation resources, $Cost^{ESS}$ is the total operation cost of storage, $Cost^{GRID}$ is the total cost of power exchange with the upstream grid.

The operation cost of the distributed generation units in the microgrid under study is presented in Eq. (4).

$$Cost^{DER} = \left\{ \sum_{S}^{SE} \Pi_s \sum_{t}^{T} \left(P_{t,s}^{PVrooftop} \lambda^{PV} + P_{t,s}^{WINDout} \lambda^{WIND} + P_t^{FU} \lambda^{FU} + P_t^{MT} \lambda^{MT} \right) + SUC^{MT} + SDC^{MT} + SUC^{FU} + SDC^{FU} \right\} \tag{4}$$

where P_t^{FU} is the output power of the fuel cell, λ^{FU} is the operation cost of the fuel cell, P_t^{MT} is the output power of the micro turbine, λ^{MT} is the operation cost of micro turbine, SUC^{MT} is the cost of turning on the microturbine, SDC^{MT} is the cost of turning off the microturbine, SUC^{FU} is the cost of turning on the fuel cell, SDC^{FU} is the cost of turning off the fuel cell.

3.1. Energy storage

The operation cost of the storage system in the microgrid under study is presented in Eq. (5).

$$Cost^{ESS} = \sum_{t}^{T} \left(P_{t,ch}^{ESS} \lambda^{ESS} \right) \tag{5}$$

where, $P_{t,dis}^{ESS}$ is the discharge power of storage, λ^{ESS} is the operation cost of the ESS.

3.2. Upstream grid

The power exchange cost with the upstream network is given in Eqs. (6)–(8).

$$Cost^{GRID} = Cost^{IMP} - Rev^{EXP} \tag{6}$$

where, $Cost^{IMP}$ indicates the amount of total cost related to the imported amount of power from the grid, while Rev^{EXP} shows the amount of obtained profit from the exported amount of power to the grid.

$$Cost^{IMP} = \sum_{S}^{SE} \Pi_s \sum_{t}^{T} \left(P_{t,s}^{IMP} \lambda_t^{IMP} \right) \tag{7}$$

where, $P_{t,s}^{IMP}$ indicates the imported amount of power from the grid, λ_t^{IMP} is the imported power price.

$$Rev^{EXP} = \sum_{S}^{SE} \Pi_s \sum_{t}^{T} \left(P_{t,s}^{EXP} \lambda_t^{EXP} \right) \tag{8}$$

where, $P_{t,s}^{EXP}$ is exported power to the grid, λ_t^{EXP} is the exported power price.

Upstream network constraints are presented in Eqs. (9)–(11).

$$P_{Min}^{IMP} I_t^{IMP} \le P_{t,s}^{IMP} \le P_{Max}^{IMP} I_t^{IMP} \tag{9}$$

where, P_{Min}^{IMP} and, P_{Max}^{IMP} indicate the corresponding limitations of the imported power from the grid and, I_t^{IMP} is a binary variable indicating the status of import of power.

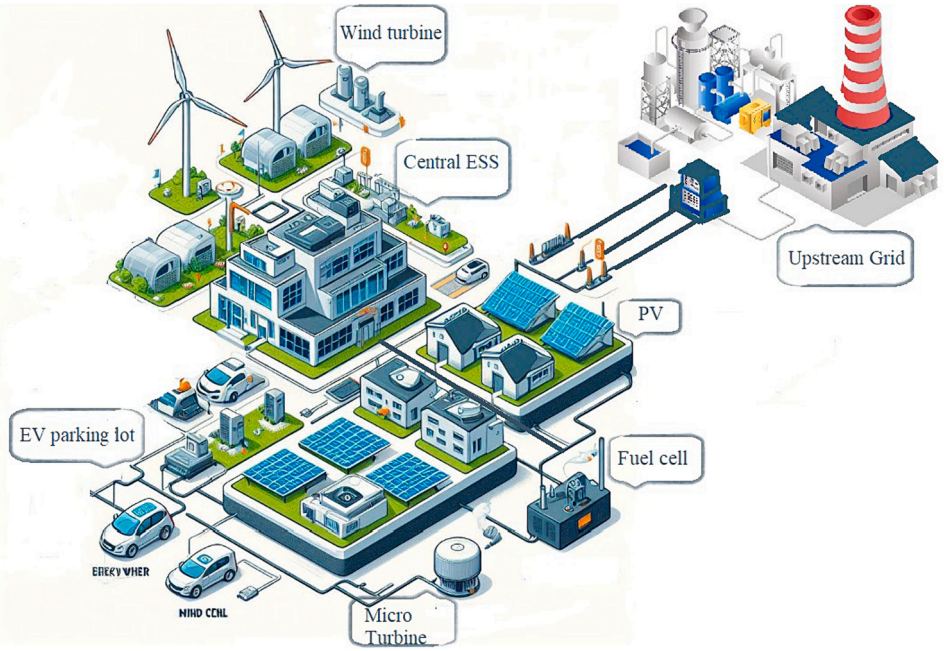

Fig. 2. The studied microgrid.

$$P_{Min}^{EXP} I_t^{EXP} \le P_{t,s}^{EXP} \le P_{Max}^{EXP} I_t^{EXP} \tag{10}$$

where, P_{Min}^{EXP} and, P_{Max}^{EXP} indicate the corresponding limitations of the exported power from the grid and, I_t^{EXP} is a binary variable indicating the status of export of power.

It should be noted that according to Eq. (11), the power cannot be imported or exported at the same time, therefore:

$$I_t^{IMP} + I_t^{EXP} \le 1 \tag{11}$$

3.3. Energy balance constraint

As a principle in any energy systems, the sum of the power produced by generation units must be equal to the demand. Electric power balance equation in the microgrid system based on solar EV, wind, micro-turbines, fuel cells and storage in Eq. (12) is given.

$$P_t^{l,DRP} + P_{t,ch}^{ESS} + P_t^{chev} + P_{t,s}^{EXP} = P_t^{MT} + P_{t,s}^{PV\ rooftop} + P_{t,s}^{WIND\ out} + P_t^{FU} + P_{t,s}^{IMP} + P_{t,dis}^{ESS} + P_t^{dchev} \tag{12}$$

where, $P_{t,s}^{PVrooftop}$ is the output power of the PV system in each scenario, $P_{t,s}^{WINDout}$ is the output power of the wind turbine in each scenario, $P_t^{l,DRP}$ is the amount of load with regarding demand response program, P_t^{chev} is the charging power of EV and P_t^{dchev} is the discharging power of EV.

3.4. Distributed generation

The generated power by the distributed generation units must be between the maximum limits of the unit. The constraints on the power production of distributed generation units are presented in Eqs. (13)–(19). Eq. (7) represents the minimum and maximum amount of the MT that can generate. The ramp-up and ramp-down limitations are also given in Eqs. (14) and (15). In addition, Eqs. (16) and (17) present the minimum up and down times of the micro-turbine, respectively. The linear model of the minimum up and down times of the unit is also indicated in (18) and (19).

$$P_{Min}^{MT} U_t^{MT} \le P_t^{MT} \le P_{Max}^{MT} U_t^{MT} \tag{13}$$

$$P_t^{MT} - P_{t-1}^{MT} \le RU\ U_t^{MT} \tag{14}$$

$$P_{t-1}^{MT} - P_t^{MT} \le RD\ U_t^{MT} \tag{15}$$

$$U_t^{MT} - U_{t-1}^{MT} \le U_{t+UP_f}^{MT} \tag{16}$$

$$U_{t-1}^{MT} - U_t^{MT} \le U_{t+DN_f}^{MT} \tag{17}$$

$$UP_f = \begin{cases} f\ f \le MUT \\ 0\ f > MUT \end{cases} \tag{18}$$

$$DN_f = \begin{cases} f\ f \le MDT \\ 0\ f > MDT \end{cases} \tag{19}$$

where, P_{Min}^{MT} and, P_{Max}^{MT} are the minimum and maximum limitations of micro turbine respectively. MUT/MDT is the minimum up/down time of micro-turbine. U_t^{MT} is a binary variable indicating if the micro-turbine is on or off. RU/DN are the ramp up/down rates of micro-turbine. DN_f/UP_f are auxiliary variable for linear modeling minimum down/up time of MT.

The output of the wind unit is calculated through Eq. (20).

$$P_{t,s}^{Wind\ out} = P_{t,s}^{Wind} \tag{20}$$

$$P_{Min}^{FU} \le P_t^{FU} \le P_{Max}^{FU} \tag{21}$$

where, P_{Min}^{FU} and, P_{Max}^{FU} are the minimum and maximum limitation power of fuel cell respectively.

3.5. Energy storage

The storage system used in the studied network is modeled by (22)–(26). The amount of energy in the battery is indicated by Eq. (22) and is limited by Eq. (23).

$$P_t^{ESS} = P_{t-1}^{ESS} + P_{t,ch}^{ESS}\eta_{ch} - P_{t,dis}^{ESS} 1 \Big/ \eta_{dis} \tag{22}$$

$$P_{Min}^{ESS} \le P_t^{ESS} \le P_{Max}^{ESS} \tag{23}$$

where, P_t^{ESS} is the capacity of the ESS, η_{ch} and, η_{dis} are charging and discharging rates of ESS respectively, P_{Min}^{ESS} and, P_{Max}^{ESS} are minimum and maximum capacity of ESS respectively.

The charging and discharging powers of ESS are constrained by (24)–(25).

$$0 \le P_{t,ch}^{ESS} \le P_{t,ch}^{Max} I_t^{ch} \tag{24}$$

$$0 \le P_{t,dis}^{ESS} \le P_{t,dis}^{Max} I_t^{dis} \tag{25}$$

Eq. (26) is employed to prevent simultaneous charge and discharge of the battery.

$$I_t^{ch} + I_t^{dis} \le 1 \tag{26}$$

This paper utilizes the TOU demand response program as an effective tool to reduce power consumption during peak times. The main purpose of this program is to modify the power consumption pattern to flatten the load curve and reduce the operation cost of energy systems.

Under TOU program, energy consumption shifts from peak to non-peak periods, which reduces total consumer payment for power consumption. This program is modeled through Eqs. (27)–(29).

$$P_t^{l,DRP} = P_t^l + DRP_t \tag{27}$$

$$-DRP_{Max} P_t^l \le DRP_t \le +DRP_{Max} P_t^l \tag{28}$$

$$\sum_t^T DRP_t = 0 \tag{29}$$

3.6. Photovoltaic (PV) system

The significant role of renewable energy resources like PV system in the operation of the power system cannot be disregarded. However, the main issue of the energy generation from the renewable energy resources is their generation fluctuations. Hence, considering an accurate model of PV system considering this characteristic is essential in order to observe more realistic results. Thus, an accurate model of PV generation in the proposed methodology is presented. In this model, the generation output of the PV system is a function that is directly related to the many real factors such solar irradiance, number of PV panels in series or parallel and the temperature of each cell. The full modeling of the PV system is presented in (30)–(32) [34], [35].

$$P_{t,s}^{pv} = P_{stc}^{pv} n_{se}^{pv} n_{pa}^{pv} \left(\frac{I_{d,s} cos\theta_\varphi + I_{dif,s}\left(\frac{1+cos\varphi}{2}\right) + \rho I_{g,s}\left(\frac{1-cos\varphi}{2}\right)}{1000} \right) \left[1 - \psi \left(T_{t,s}^c - 25 \right) \right] \tag{30}$$

In (30), P_{stc}^{pv} indicates output of the power of the PV system at the standard condition and the maximum power point. Moreover, n_{se}^{pv} shows the PV panel numbers that are installed in series and n_{pa}^{pv} indicates the PV panel numbers that are installed in parallel. The direct normal irradiance and the incidence angle of solar radiation on a tilted surface are modeled through $I_{d,s}$ and θ_φ, respectively. While $I_{dif,s}$ is diffuse horizontal irradiance, φ shows the tilted angle, the surrounding reflection is shown

by ρ, $I_{g,s}$ is the global horizontal irradiance, ψ is the coefficient related to the PV system's temperature and finally, temperature of cells in the PV system is addressed by $T^{c}_{t,s}$. It should be noted that the cells temperature has a direct relation with the temperature of ambient that is represented in (31). In this equation, the ambient and the cell nominal temperatures are denoted by $T^{a}_{t,s}$ and NCT.

$$T^{c}_{t,s} = T^{a}_{t,s} + \left(\frac{I_{d,s} cos\theta_{\varphi} + I_{dif,s}\left(\frac{1+cos\varphi}{2}\right) + \rho I_{g,s}\left(\frac{1-cos\varphi}{2}\right)}{800} \right)(NCT - 20) \quad (31)$$

It should be noted that the PV system power generation should be limited according to the its legal nominal range as declared in (32).

$$P^{PV}_{t,s} \leq P^{nppt}_{t,max} \quad (32)$$

3.7. Electric vehicle model

The proposed integrated EV model is mathematically formulated in (33)–(35). The energy consumption process can be optimized in RCs through optimal charge and discharge procedure of EVs. While there are some restrictions that are required to be considered in order to make the model as realistic as possible such as EVs availability, charging/discharging ratios and etc. Thus, in the proposed integrated EV model, total charged power of EV is addressed in (33). According to this equation, the total charged power of EV cannot be greater than maximum charging capacity if it is available for the EV to be charged. Similarly, in (34), the total discharged power of EV cannot be greater than maximum discharging capacity if it is available for the EV to be discharged. It should be mentioned that it is not possible for the EV to be charged and discharged simultaneously. Therefore, Eq. (35) is being employed to model this limitation. B^{ch}_{t} and B^{dch}_{t} are binary variables which indicate that if the EV is in charging or discharging mode, respectively. M_t binary variable, which is 1 if the EV is in the PL; otherwise, 0.

$$P^{chev}_{t} \leq P^{chev}_{max} B^{ch}_{t} M_t \quad (33)$$

$$P^{dchev}_{t} \leq P^{dchev}_{max} B^{dch}_{t} M_t \quad (34)$$

$$B^{ch}_{t} + B^{dch}_{t} \leq M_t \quad (35)$$

There is an important concept in the EV system that is state of charge (SOC) of the EV. SOC is highly dependent on the situation of the EV in the previous time interval and charging or discharging modes. In order to consider SOC in the proposed EV system, constraints (31)–(35) have been taken into account. In Eq. (31), the SOC of EV is denoted by SOC_t. The charging and discharging ratios of EV is denoted by η^{chev}_{t} and η^{dchev}_{t}, respectively.

$$SOC_t = SOC_{t-1} + P^{chev}_{t}\eta^{chev}_{t} - \frac{P^{dchev}_{t}}{\eta^{dchev}_{t}} \quad (36)$$

The SOC of EV has a capacity which cannot surpass or be less than this range which is presented in (32).

$$SOC_{Min} \leq SOC_t \leq SOC_{Max} \quad (37)$$

The arrival and departure time conditions of the EVs from the charging station are expressed in (38)–(40). To make our model more comprehensive, various driving patterns are essential to be considered. To this end, a scenario-based approach has been taken into account. The scenario generation method is considered based on a stochastic nature of the values of SOCs upon arrival time of EVs to the charging station. In Eq. (38), the SOC of EV upon the arrival time is denoted by SOC^{Arive}_{t} and the maximum correlated value is indicated by SOC^{Arive}_{Max}. Finally, SOC^{Dep}_{t} and $SOC^{Dep}_{desired}$ terms are addressing the SOC of EV upon departure and desired SOC of EV upon departure.

$$SOC^{Arrive}_{t} \leq SOC^{Arrive}_{Max} \quad (38)$$

$$SOC^{Dep}_{t} \leq SOC^{Dep}_{desired} \quad (39)$$

$$SOC^{Dep}_{desired} = SOC_{Max} \quad (40)$$

In this part, the uncertainty of the load is taken into account. The procedure of the proposed stochastic-IGDT is shown in a flowchart, i.e., Fig. 3. In the schematic, the cost deviation factor (σ), representing the level of risk or uncertainty in the operation cost, is required to updated iteratively for different risk levels. The deviation factor is a value between 0 and 1. Depending on the chosen strategy (Risk-averse or Risk-seeker), the model optimizes the operation of the microgrid by maximizing the uncertain robust region (for risk-averse) or the uncertain opportunistic region (for risk-seeker). Therefore, IGDT robustness strategy is suitable for risk-averse decision-makers and IGDT opportunity strategy is suitable for risk-seeking decision-makers.

Thus, the problem formulation for the robustness strategy is presented as follows:

$$Max\ \alpha \quad (41)$$

$$s.t. \quad (42)$$

$$Max\left\{OC^{*} = \left(Cost^{DER} + Cost^{ESS} + Cost^{GRID}\right)\right\} \quad (43)$$

$$OC^{*} \leq OC_{Cr} = (1+\sigma)OC_0 \quad (44)$$

$$(1-\alpha)\widetilde{P}^{Load}_{t} \leq P^{Load}_{t} \leq (1+\alpha)\widetilde{P}^{Load}_{t} \quad (45)$$

$$(2) - (40) \quad (46)$$

where the objective function of this strategy is maximizing the horizon of the uncertain parameter, i.e., α, while assuring the decision-maker that the cost of the model will not be higher than the critical cost, OC_{Cr}. This critical cost is calculated through the objective function of the deterministic stage and the deviation factor (σ). The level of risk-averseness is determined through the deviation factor which is a value between 0 and 1 as an input parameter. For higher protection against the uncertain parameter, the higher values of σ σ should be selected. Eq. (40) indicates that the worse-case scenario of the load uncertainty occurs when $P^{Load}_{s.t} = (1+\alpha)\widetilde{P}^{Load.}_{s.t}$

. The observed value for load is denoted by P^{load}_{t} and $\widetilde{P}^{load}_{t}$ is the expected values for the uncertain parameter. The rest of the constraints remain unchanged similar to the deterministic stage.

In addition, the risk-seeking decision-makers can choose IGDT opportunity strategy to evaluate the possibility of reaching lower cost if the favorable deviations in the uncertain parameter happen. To this end, the minimum horizon of uncertainty, i.e., β should be find through the optimization model that is presented as follows:

$min\ \beta$ (47)$s.t.$

$$min\ OC^{*} = \left(Cost^{DER} + Cost^{ESS} + Cost^{GRID}\right) \quad (48)$$

$$OC^{*} \leq OC_{Tr} = (1-\sigma)OC_0 \quad (49)$$

$$(1-\beta)\widetilde{P}^{Load}_{t} \leq P^{Load}_{t} \leq (1+\beta)\widetilde{P}^{Load}_{t} \quad (50)$$

$$(2) - (40) \quad (51)$$

In the IGDT opportunity strategy, the objective function is finding the minimum horizon of the uncertainty that if the load (uncertain parameter) deviates favorably, lower or equal costs than the target cost, denoted by OC_{Cr} can be achieved by the risk-seeking decision-maker. The target cost is calculated through $OC_{Tr} = (1-\sigma)OC_0$, where OC_0 is the objective function of the deterministic problem formulation and σ is the deviation

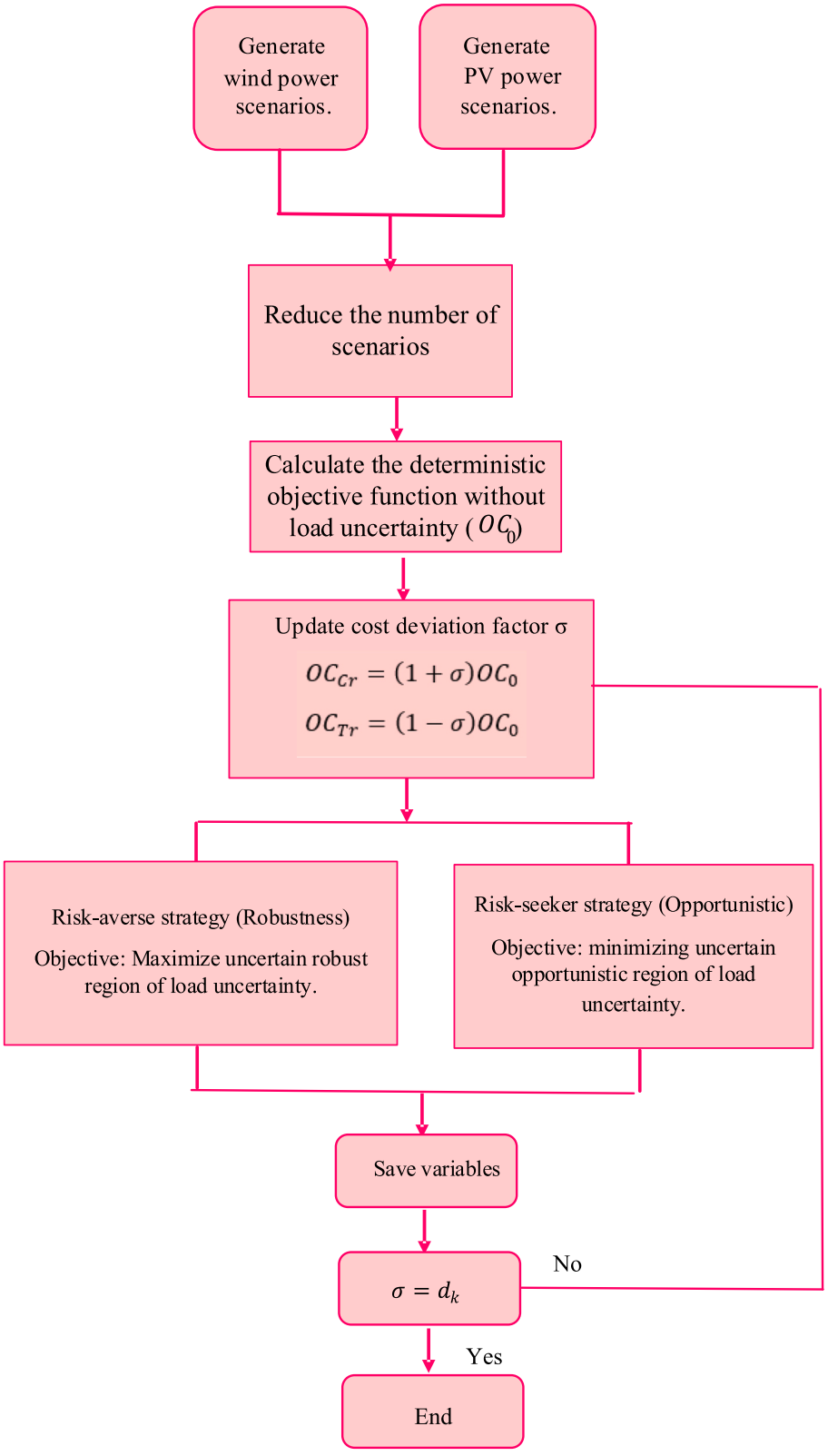

Fig. 3. The schematic of the proposed stochastic-IGDT approach.

factor that shows the risk level that is explained in the above section. In order to be able to reach to the lower costs than the target cost, it is required that the observed values of the uncertain parameter be equal to the best-case scenario, i.e., $P_t^{load} = (1-\beta)\widetilde{P}_t^{load}$. The rest of the constraints remain unchanged similar to the deterministic stage.

4. Case study

4.1. Data preparation

Technical limitations and prices and operation costs of distributed

Table 2
Technical limitations and prices and operation costs of distributed generation units.

Micro turbine	Unit	Value
SUC^{MT}	€ct	0.96
SDC^{MT}	€ct	0.96
P^{MT}_{Min}	kW	6
P^{MT}_{Max}	kW	30
λ^{MT}	€/kWh	0.457

Fuel cell	Unit	Value
SUC^{FU}	€ct	1.65
SDC^{MT}	€ct	1.65
P^{FU}_{Min}	kW	3
P^{FU}_{Max}	kW	30
λ^{FU}	€/kWh	0.294

PV system	Unit	Value
λ^{PV}	€ct/kWh	2.584
P^{pv}_{stc}	kW	0.26
n^{pv}_{se}	–	12
n^{pv}_{pa}	–	1
NOCT	°C	46
ρ	–	0.2
α	°C	0.0045

Upper network	Unit	Value
P^{IMP}_{Min}	kW	−30
P^{IMP}_{Max}	kW	30
P^{EXP}_{Min}	kW	−30
P^{EXP}_{Max}	kW	30

Wind	Unit	Value
λ^{WIND}	(€ct/kWh)	1.073

ESS	Unit	Value
λ^{ESS}	(€ct/kWh)	0.38
η_{ch}	%	0.9
η_{dis}	%	0.9
P^{ESS}_{Max}	kW	30
P^{ESS}_{Min}	kW	−30

EV	Unit	Value
η^{chev}_{t}	%	90
η^{dchev}_{t}	%	80
P^{chev}_{Max}	kW	2.3
P^{dchev}_{Max}	kW	2.3
SOC_{Min}	kWh	0.6
SOC_{Max}	kWh	3
SOC^{Arive}_{Max}	kWh	0.6
$SOC^{Dep}_{desired}$	kWh	2.3

generation units in the microgrid are listed in Table 2 [35], [36].

4.2. Simulation results

The proposed model is formulated as mixed-integer non-linear programming (MINLP) problem in mathematical-based tool, GAMS software. The proposed model is solved using both SBB and DICOPT commercial solvers. Some of the most important and significant results of the simulated model is demonstrated for different risk levels including risk-averse, risk-neutral and risk-seeker decision maker. The generated amount of power by PV unit is depicted in Fig. 4. The uncertainty of PV, its amount is constant in all conditions. According to the result, it is obvious that as expected, this generation is directly related to solar radiation and it reaches its maximum during mid-day for several scenarios that are generated through the Monte-Carlo approach.

Fig. 5 shows the degree of uncertainty studied against different critical costs. As can be seen, when uncertainty is not considered $\sigma = 0$, the critical cost is equal to the total cost obtained in deterministic mode. However, by increasing the amount of σ, which leads to an increase in the critical cost $OC_{Cr} = (1 + \sigma)OC_0$, a larger amount of α is obtained, so if the decision maker wants to increase the amount of risk aversion, it must choose larger σ, which leads to an increase in the critical cost. However, it is possible to achieve a higher uncertainty interval, for example, when $\sigma = 0.3$ is chosen, the critical cost is equal to €849.226, which is obtained by α from the solution of the model, it is equal to 0.078, that is, if the observed loads values deviate 7.8 % higher than the expected values, the decision maker is sure that the final total cost will not be higher than €849.226.

The next figure shows the amount of uncertainty of the load against different target costs in a risk-seeking strategy. According to Fig. 6, when the uncertainty is not considered, the amount of the total cost is equal to the cost obtained in deterministic mode that is €654.02, but with the increase of σ, the target cost decreases, which is desirable for a decision maker with high risk-seeking attitude: $OC_{Ta} = (1 - \sigma)OC_0$. In this formula, σ is the risk level indicator which is a number between zero and one. The closer to zero, the less willing the decision maker is to take risks, and vice versa. For instance, when $\sigma = 0.3$ is selected, the target price is equal to €457.88, which in this case, the horizon of uncertainty, i.e. β is equal to 0.083, which means that if the amount of observed loads is at least 8.3 % lower than the amount of expected loads, it is possible for the decision maker to achieve to the target cost equal to €457.88.

The discharged power of EV to the microgrid in the studied 24 h is shown in Fig. 7. As depicted in figure, the amount of power when the decision maker is risk taker is maximum. As the risk-seeker decision maker desire to gain more profit, hence the amount of the discharged power through EV to the microgrid is higher than others.

The energy of storage in risk-averse, risk-neutral and risk-seeker modes is depicted in Fig. 8. In the risk-averse mode, the ESS stores the maximum amount of energy. This is expected as the decision maker wants to avoid any uncertainty that could lead to system loss. The high storage level acts as a buffer, ensuring that there is always enough energy to meet demand, even if power generation fluctuates. However, the amount of stored energy decreases around mid-day. This could be due to the increased power generation from the PV unit during this time, reducing the need for energy from storage. While the risk-seeking mode has the least amount of energy storage. The decision maker is willing to take on more risk for potential higher returns. This could mean relying more on utilization of real-time power generation rather than stored energy to have a positive impact on reaching to the target costs while accepting the risk.

Fig. 9 presents the results of the generated power through micro-turbine. It can be seen that the decision maker is prioritizing stability and risk mitigation over potential high returns in power generation from the micro-turbine. This is evident from the higher power production in the risk-averse mode compared to the risk-seeker mode. In the risk-averse mode, the decision maker opts to use the micro-turbine more frequently, thereby ensuring a steady and reliable power supply which can minimize the risk of load loss in the microgrid. On the other hand, the risk-seeker mode seems to be used less frequently, resulting in lower power production. This could be due to the decision maker's willingness to take on more risk for the potential of achieving much lower final costs.

As highlighted in the problem formulation section, the proposed model integrates the demand response program (DRP) to effectively

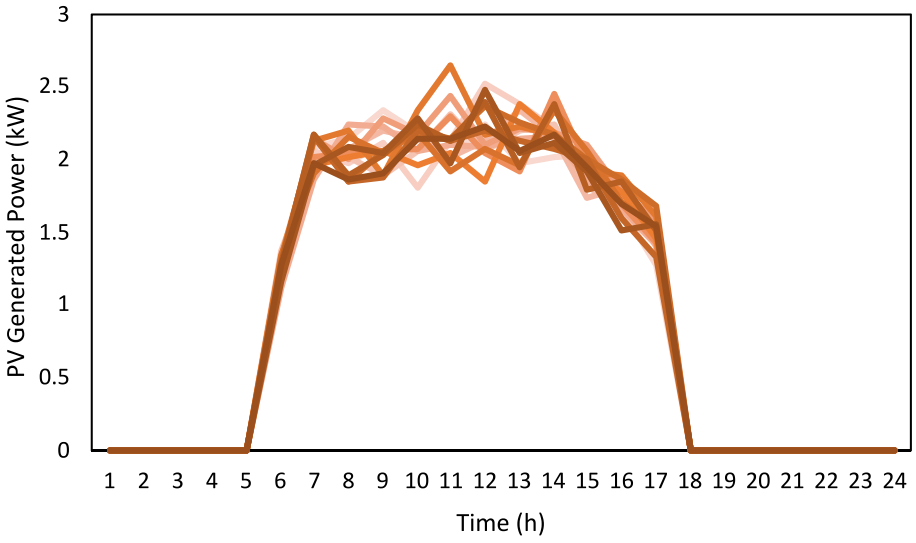

Fig. 4. The amount of generated power by PV unit.

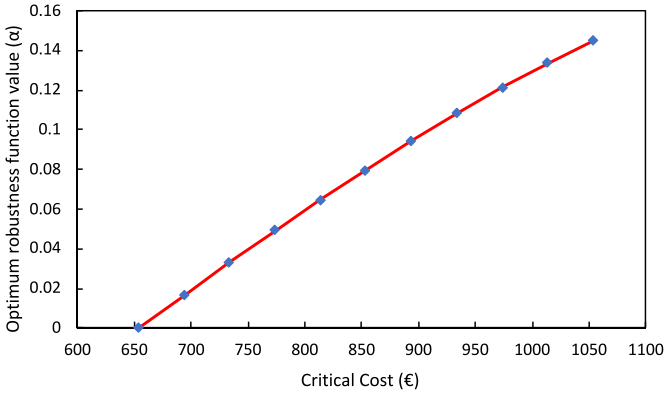

Fig. 5. The optimum robustness function value for various critical costs in a risk-averse strategy.

minimize costs associated with the objective function. Fig. 10 visually represents the load variations before and after the implementation of the DRP. Notably, the initial load curve exhibits two prominent peaks at 10 AM and 7 PM. However, the introduction of the DRP brings about a noticeable shift in the consumption pattern, resulting in reduced energy usage during peak hours. Moreover, the figure exemplifies the application of the DRP in both risk-averse and risk-taking strategies. In the risk-

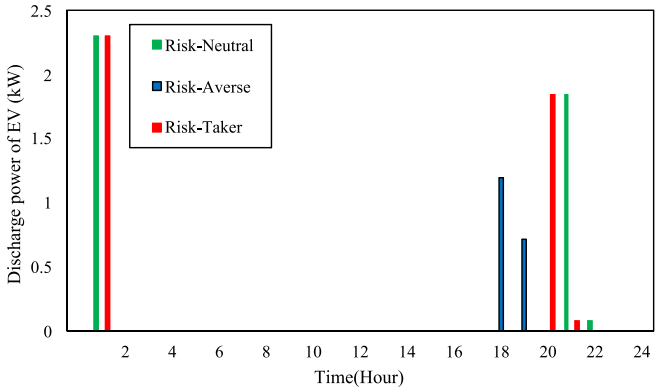

Fig. 7. Discharge power of the EV for three different risk levels: risk-averse, risk-neutral and risk-seeker.

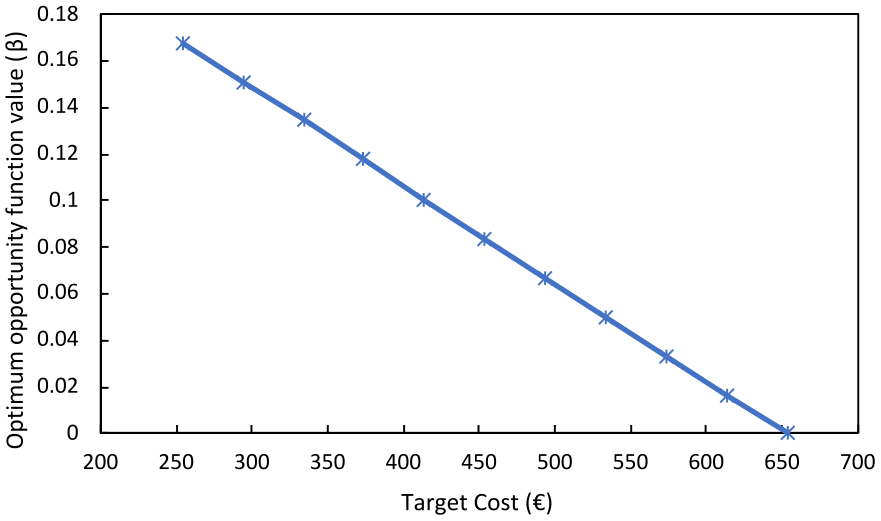

Fig. 6. The optimum opportunity function value for various critical costs in a risk-seeking strategy.

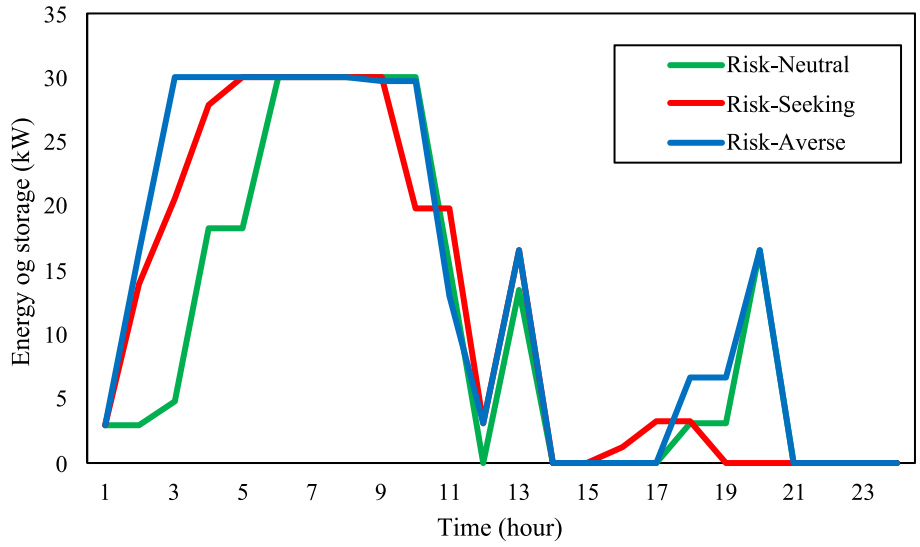

Fig. 8. The amount of stored energy in the energy storage with three different risk levels: risk-averse, risk-neutral and risk-seeker.

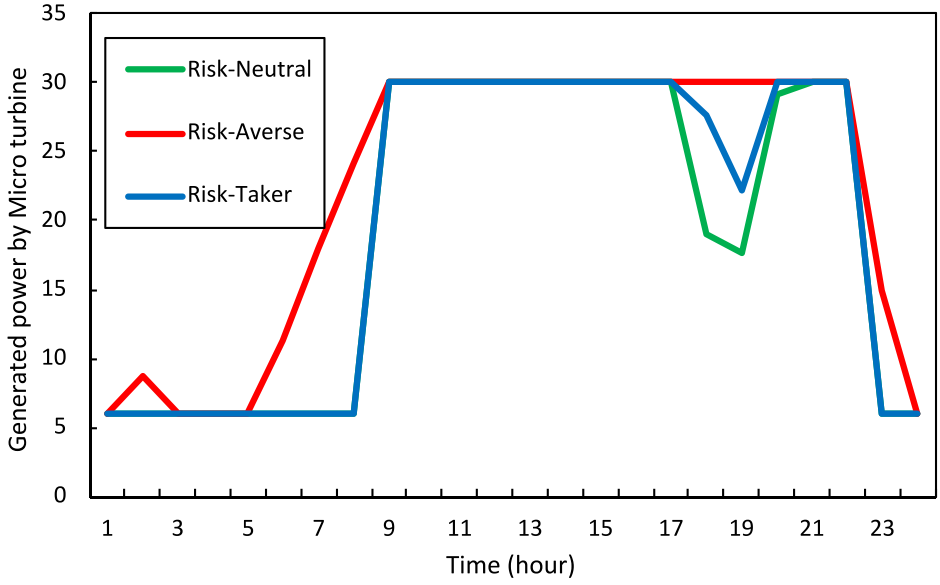

Fig. 9. The amount of generated power of the micro-turbine for three different modes: risk-averse, risk-neutral and risk-seeker.

averse mode, decision makers opt to increase consumption in order to mitigate the risk of a substantial discrepancy between power supply and demand. Nonetheless, this increase in consumption subsequently leads to higher overall costs. In contrast, in the risk-taking strategy, decision makers willingly looking for the potential of reducing consumption during the peak period and increase on the off-peak period in order to use the advantage of lower energy supplying costs, thus it can desire to achieve a more pronounced reduction in the final cost of the objective function through the implementation of the DRP.

Another parameter that is required to be considered in this modeling is the cost that the risk management model imposes on the system. For this purpose, the cost of implementing the robust strategy and the opportunity strategy are presented in Figs. 11 and 12. to calculate this cost the robust strategy is equal to $R_{cost} = OC_0 - OC_{cr}(\sigma)$ and for opportunity strategy is equal to $O_{cost} = OC_0 - OC_{Tr}(\sigma)$ the objective function is equal to OC_0 when uncertainty is not considered and the objective function is equal to $OC_r(\sigma)$ when the uncertainty parameter of the observed load is equal to the expected value. In this case, for different σ function, different objectives are obtained which difference OC_0 is equal to R_{cost}, in the same way O_{cost} is calculated for the opportunity strategy. The figures provide clear evidence that as the decision-making stage aims to enhance the model's resilience to load uncertainty or pursue a more opportunistic approach, the cost of risk management also increases. However, it is crucial to acknowledge that there is a point where the cost of implementing risk management becomes prohibitively high, rendering it ineffective for decision making.

In this part, the variations in microgrid costs under various observed scenarios that we considered for our uncertain parameter, load. For this purpose, manipulated load forecasts have been employed to generate simulated loads, which are then used to analyze the effects of deviations in observed loads from forecasted loads. The potential cost for the operator using the robust model, represented by OC*, is determined using these simulated loads. The robust schedules are established by solving the models with an arbitrary value of σ = 0.42, taking into account the depicted forecast loads. In this scenario, the robustness parameter α is set at 0.108. If the hourly forecast errors are kept below 10.8 % for the robust model, it ensures that the maximum cost is (1 + 0.42) OC_0 = €934.

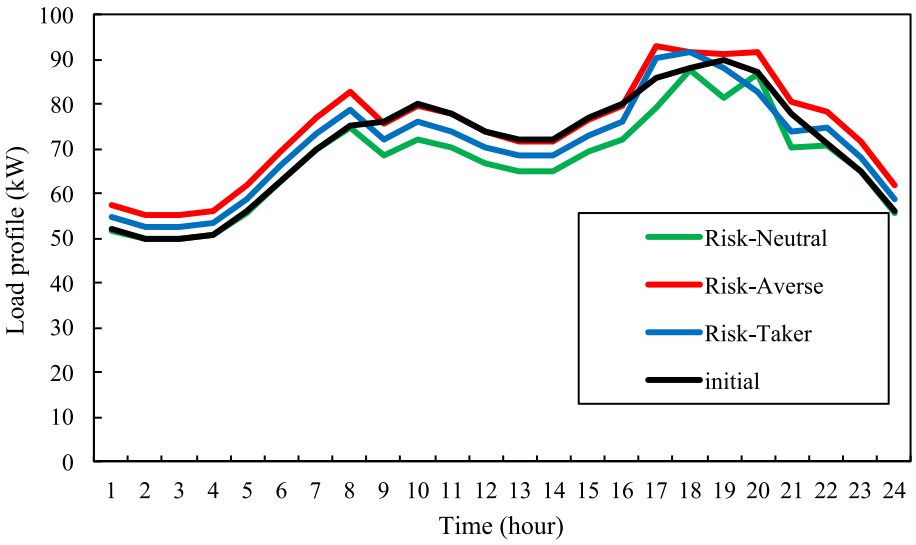

Fig. 10. The impact of DRP on the load profile for three different strategies: risk-averse, risk-neutral and risk-seeker vs. the initial load pattern.

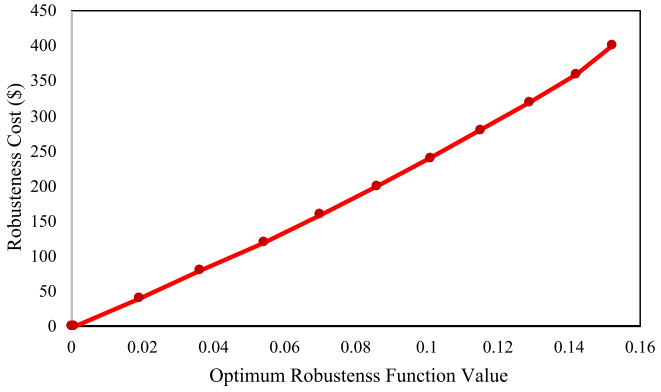

Fig. 11. The robustness cost for different values of the horizon of the uncertainty of the load parameter.

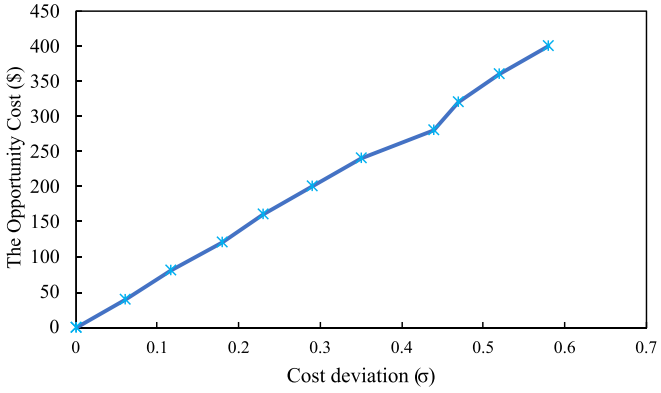

Fig. 12. The robustness cost for different values of the horizon of the uncertainty of the load parameter.

We are considering three different scenarios for observed load pattern. In the 1st scenario, the values of the simulated loads exceed those of the forecasted loads, yet they remain within the robustness region, $\alpha = 0.108$. Then, in the 2nd scenario, the simulated loads are distributed randomly, but they are still confined within the robustness region. Finally, at the last scenario, at hours 19 and 20, the simulated loads significantly surpass the upper limit of the robustness region, reaching 1100 kW. During the remaining hours, the load values are randomly generated exceeding their forecasted values but still within the robustness region.

Table 3 presents the results for OC* based on the previously mentioned three scenarios. Hours 19 and 20 in scenario 3 have been specifically selected to study the effect of load spikes on the proposed IGDT-based problem. The table reveals that for the first two scenarios, where the loads are within the robustness region, the critical cost of the robust model, i.e., OC* $<$ €934, is not exceeded. However, for scenario 3, where some of the load exceeds the robustness region, the critical cost is not guaranteed. This is due to the fact that the loads outside the robustness region are significantly higher than the forecasted values, resulting in the critical cost not being achieved.

Most of the similar models considering uncertain parameters are modeled on a scenario-based approaches. These methods assume that the uncertain parameter is characterized by a specific probability distribution function (PDF, such as a normal PDF, and the optimization problem is solved using scenario generation (creating scenarios for each probability). The primary objective in these problems is to minimize cost across different scenarios. However, in the current paper, it is assumed that no PDF is available for the load. Thus, the problem is not solved with scenario-based methods for the load uncertainty, and the main goal is not to minimize cost but to identify the highest load variations, such that the scheduling cost is less than the operator's expected value. As a result, the method proposed in this paper cannot be compared with any other methods presented. As highlighted in the paper, the IGDT method would be extremely beneficial in problems with uncertain parameters that are associated with incomplete information. The proposed model in this paper is subject to load uncertainty with incomplete information, as it is not possible to use any specific PDF for load demand. While the uncertainty posed from the renewable generations are modeled through stochastic programming. Therefore, proposing a stochastic-IGDT approach can be beneficial to address both types of the uncertain parameters including with some information (wind and solar generation) and a parameter without complete information (load) [37].

Table 3
After-the-fact analysis using simulated loads.

Load scenario (kW)	OC* (€)
1st scenario	913
2nd scenario	854
3rd scenario	1121

5. Conclusion

Electrification and dependence on reliable electricity supply in different areas requires increased resiliency supporting technical solutions from the energy systems with simultaneous consideration of economic aspects as well. One of the most proper solutions to this end is utilization of microgrids in the energy systems. In this paper, a stochastic optimal operation of microgrid including renewable recourses, energy storage and DR programs has been proposed. The studied microgrid included PV system, wind system, micro-turbine, fuel cell, EV, and energy storage. The load was considered as the uncertain parameter and its uncertainty has been addressed through the information-gap decision theory approach. Furthermore, the uncertainties of wind and PV units are modeled with a scenario-based approach.

Three different strategies were studied i.e. risk-averse, risk-neutral and risk-seeker mode. The impacts of risk-averseness or risk-seeking of the decision maker affect the system operation. For instance, the amount of energy storage when the decision maker takes risk averse strategy is the maximum as expected. Since in this mode, it is desired to avoid any uncertainty that leads to loss to the system. Therefore, it will try to store its maximum capacity of energy to this end. Moreover, the study demonstrates the DRP's use in both risk-averse and risk-taking approaches, affecting consumption and overall costs. Decision makers can mitigate risks through increased consumption or seek cost reduction by reducing consumption using the DRP. Moreover, it is shown that the decision-maker's risk attitude has a significant impact on the microgrid's costs. When the decision-maker adopts a risk-averse strategy, the final total costs will be higher as they tend to pay more to balance the power from DERs and the upstream network, making the system more robust against the uncertainty of load consumption. On the other hand, if the decision-maker adopts a risk-taking strategy, the final costs are lower as they gain benefits through a possible decrease in the load, thus reducing the total costs of the microgrid which is dependent on the total consumed load. Therefore, the decision-maker's risk attitude directly influences the operational costs of the microgrid. Finally, the importance of considering the cost imposed by the risk management model is essential to be considered. As results demonstrated, if robust or opportunistic approach is pursued, there would be a risk management cost that increases. Thus, the decision-maker should consider this cost upon choosing the level of risk-averseness or risk-seeking. An after-the-fact analysis approach is also employed to demonstrate the effectiveness of the proposed model. Based on the findings of this study, future work can focus on evaluating the impacts of utilized technologies such as ESS, EV, RESs on the resilience of microgrids under different risk profiles.

CRediT authorship contribution statement

Sahar Seyedeh-Barhagh: Conceptualization, Data curation, Investigation, Methodology, Visualization, Writing – original draft. **Mehdi Abapour:** Formal analysis, Methodology, Writing – review & editing. **Behnam Mohammadi-Ivatloo:** Formal analysis, Validation, Writing – review & editing. **Miadreza Shafie-Khah:** Validation, Writing – review & editing. **Hannu Laaksonen:** Funding acquisition, Project administration, Supervision, Validation, Writing – review & editing.

Declaration of competing interest

The authors declare that they have no known competing financial interests or personal relationships that could have appeared to influence the work reported in this paper.

Data availability

No data was used for the research described in the article.

Refrences

[1] R. Razipour, S.M. Moghaddas-Tafreshi, P. Farhadi, Optimal management of electric vehicles in an intelligent parking lot in the presence of hydrogen storage system, J. Energy Storage (2019), https://doi.org/10.1016/j.est.2019.02.001.

[2] J. Jannati, D. Nazarpour, Optimal energy management of the smart parking lot under demand response program in the presence of the electrolyser and fuel cell as hydrogen storage system, Energy Convers. Manag. (2017), https://doi.org/10.1016/j.enconman.2017.02.030.

[3] J. Jannati, D. Nazarpour, Optimal performance of electric vehicles parking lot considering environmental issue, J. Clean. Prod. (2019), https://doi.org/10.1016/j.jclepro.2018.09.222.

[4] R. Figueiredo, P. Nunes, M.C. Brito, The feasibility of solar parking lots for electric vehicles, Energy (2017), https://doi.org/10.1016/j.energy.2017.09.024.

[5] J. Jannati, D. Nazarpour, Multi-objective scheduling of electric vehicles intelligent parking lot in the presence of hydrogen storage system under peak load management, Energy (2018), https://doi.org/10.1016/j.energy.2018.08.098.

[6] P. Nunes, R. Figueiredo, M.C. Brito, The use of parking lots to solar-charge electric vehicles, Renew. Sust. Energ. Rev. (2016), https://doi.org/10.1016/j.rser.2016.08.015.

[7] M. Shepero, J. Munkhammar, J. Widén, J.D.K. Bishop, T. Boström, Modeling of photovoltaic power generation and electric vehicles charging on city-scale: a review, Renew. Sust. Energ. Rev. (2018), https://doi.org/10.1016/j.rser.2018.02.034.

[8] U.C. Chukwu, S.M. Mahajan, V2G parking lot with pv rooftop for capacity enhancement of a distribution system, IEEE Trans. Sustain. Energy (2014), https://doi.org/10.1109/TSTE.2013.2274601.

[9] M. Nasir, A. Rezaee Jordehi, M. Tostado-Véliz, S.A. Mansouri, E.R. Sanseverino, M. Marzband, Two-stage stochastic-based scheduling of multi-energy microgrids with electric and hydrogen vehicles charging stations, considering transactions through pool market and bilateral contracts, Int. J. Hydrog. Energy (Mar. 2023), https://doi.org/10.1016/J.IJHYDENE.2023.03.003.

[10] G.J. Osório, et al., Modeling an electric vehicle parking lot with solar rooftop participating in the reserve market and in ancillary services provision, J. Clean. Prod. (2021), https://doi.org/10.1016/j.jclepro.2021.128503.

[11] M.K. Daryabari, R. Keypour, H. Golmohamadi, Stochastic energy management of responsive plug-in electric vehicles characterizing parking lot aggregators, Appl. Energy (2020), https://doi.org/10.1016/j.apenergy.2020.115751.

[12] A.S. Godazi Langeroudi, M. Sedaghat, S. Pirpoor, R. Fotouhi, M.A. Ghasemi, Risk-based optimal operation of power, heat and hydrogen-based microgrid considering a plug-in electric vehicle, Int. J. Hydrog. Energy (2021), https://doi.org/10.1016/j.ijhydene.2021.06.062.

[13] M. Tostado-Véliz, S. Kamel, H.M. Hasanien, P. Arévalo, R.A. Turky, F. Jurado, A stochastic-interval model for optimal scheduling of PV-assisted multi-mode charging stations, Energy (2022), https://doi.org/10.1016/j.energy.2022.124219.

[14] X. Fang, Y. Wang, W. Dong, Q. Yang, S. Sun, Optimal energy management of multiple electricity-hydrogen integrated charging stations, Energy 262 (Jan. 2023) 125624, https://doi.org/10.1016/J.ENERGY.2022.125624.

[15] Y. Wu, J. Zhang, A. Ravey, D. Chrenko, A. Miraoui, Real-time energy management of photovoltaic-assisted electric vehicle charging station by markov decision process, J. Power Sources (2020), https://doi.org/10.1016/j.jpowsour.2020.228504.

[16] A. Azarhooshang, D. Sedighizadeh, M. Sedighizadeh, Two-stage stochastic operation considering day-ahead and real-time scheduling of microgrids with high renewable energy sources and electric vehicles based on multi-layer energy management system, Electr. Power Syst. Res. (2021), https://doi.org/10.1016/j.epsr.2021.107527.

[17] S.E. Ahmadi, S.M. Kazemi-Razi, M. Marzband, A. Ikpehai, A. Abusorrah, Multi-objective stochastic techno-economic-environmental optimization of distribution networks with G2V and V2G systems, Electr. Power Syst. Res. (2023), https://doi.org/10.1016/j.epsr.2023.109195.

[18] S. Guner, A. Ozdemir, Distributed storage capacity modelling of EV parking lots, in: ELECO 2015 - 9th International Conference on Electrical and Electronics Engineering, 2016, https://doi.org/10.1109/ELECO.2015.7394580.

[19] A. Mohamed, V. Salehi, T. Ma, O. Mohammed, Real-time energy management algorithm for plug-in hybrid electric vehicle charging parks involving sustainable energy, IEEE Trans. Sustain. Energy (2014), https://doi.org/10.1109/TSTE.2013.2278544.

[20] S. Aghajani, M. Kalantar, A cooperative game theoretic analysis of electric vehicles parking lot in smart grid, Energy (2017), https://doi.org/10.1016/j.energy.2017.07.006.

[21] A.K. Mathur, C. Teja S, P.K. Yemula, Optimal charging schedule for electric vehicles in parking lot with solar power generation, in: 2018 IEEE Innovative Smart Grid Technologies - Asia (ISGT Asia), IEEE, May 2018, pp. 611–615, https://doi.org/10.1109/ISGT-Asia.2018.8467916.

[22] A.R. Bhatti, et al., Optimized sizing of photovoltaic grid-connected electric vehicle charging system using particle swarm optimization, Int. J. Energy Res. 43 (1) (Jan. 2019) 500–522, https://doi.org/10.1002/er.4287.

[23] S.E. Ahmadi, S.M. Kazemi-Razi, M. Marzband, A. Ikpehai, A. Abusorrah, Multi-objective stochastic techno-economic-environmental optimization of distribution networks with G2V and V2G systems, Electr. Power Syst. Res. 218 (May 2023), https://doi.org/10.1016/j.epsr.2023.109195.

[24] M. Nodehi, A. Zafari, M. Radmehr, A new energy management scheme for electric vehicles microgrids concerning demand response and reduced emission, Sustain. Energy Grids Netw. 32 (Dec. 2022) 100927, https://doi.org/10.1016/J.SEGAN.2022.100927.

[25] Y. Wu, J. Zhang, A. Ravey, D. Chrenko, A. Miraoui, Real-time energy management of photovoltaic-assisted electric vehicle charging station by markov decision process, J. Power Sources 476 (Nov. 2020) 228504, https://doi.org/10.1016/J.JPOWSOUR.2020.228504.
[26] M. Wang, X. Dong, Y. Zhai, Optimal configuration of the integrated charging station for PV and hydrogen storage, Energies 14 (21) (Oct. 2021) 7087, https://doi.org/10.3390/EN14217087, 2021, Vol. 14, Page 7087.
[27] M. Tostado-Véliz, A. Rezaee Jordehi, D. Icaza, S.A. Mansouri, F. Jurado, Optimal participation of prosumers in energy communities through a novel stochastic-robust day-ahead scheduling model, Int. J. Electr. Power Energy Syst. 147 (May 2023) 108854, https://doi.org/10.1016/J.IJEPES.2022.108854.
[28] H. Golmohamadi, Stochastic energy optimization of residential heat pumps in uncertain electricity markets, Appl. Energy 303 (Dec. 2021) 117629, https://doi.org/10.1016/J.APENERGY.2021.117629.
[29] G.J. Osório, et al., Modeling an electric vehicle parking lot with solar rooftop participating in the reserve market and in ancillary services provision, J. Clean. Prod. 318 (Oct. 2021) 128503, https://doi.org/10.1016/J.JCLEPRO.2021.128503.
[30] M. Nasir, A. Rezaee Jordehi, M. Tostado-Véliz, S.A. Mansouri, E.R. Sanseverino, M. Marzband, Two-stage stochastic-based scheduling of multi-energy microgrids with electric and hydrogen vehicles charging stations, considering transactions through pool market and bilateral contracts, Int. J. Hydrog. Energy 48 (61) (Jul. 2023) 23459–23497, https://doi.org/10.1016/J.IJHYDENE.2023.03.003.
[31] Y. Ben-Haim, Info-gap Decision Theory: Decisions Under Severe Uncertainty, 2006.
[32] M. Majidi, B. Mohammadi-Ivatloo, A. Soroudi, Application of information gap decision theory in practical energy problems: a comprehensive review, Appl. Energy 249 (Sep. 2019) 157–165, https://doi.org/10.1016/J.APENERGY.2019.04.144.
[33] S. Liao, H. Liu, B. Liu, H. Zhao, M. Wang, An information gap decision theory-based decision-making model for complementary operation of hydro-wind-solar system considering wind and solar output uncertainties, J. Clean. Prod. 348 (May 2022) 131382, https://doi.org/10.1016/J.JCLEPRO.2022.131382.
[34] S. Seyyedeh Barhagh, M. Abapour, B. Mohammadi-Ivatloo, Optimal scheduling of electric vehicles and photovoltaic systems in residential complexes under real-time pricing mechanism, J. Clean. Prod. 246 (Feb. 2020) 119041, https://doi.org/10.1016/j.jclepro.2019.119041.
[35] B.P. Numbi, S.J. Malinga, Optimal energy cost and economic analysis of a residential grid-interactive solar PV system- case of eThekwini municipality in South Africa, Appl. Energy (2017), https://doi.org/10.1016/j.apenergy.2016.10.048.
[36] A.A. Moghaddam, A. Seifi, T. Niknam, M.R. Alizadeh Pahlavani, Multi-objective operation management of a renewable MG (micro-grid) with back-up micro-turbine/fuel cell/battery hybrid power source, Energy (2011), https://doi.org/10.1016/j.energy.2011.09.017.
[37] M. Charwand, A. Ahmadi, A.M. Sharaf, M. Gitizadeh, A. Esmaeel Nezhad, Robust hydrothermal scheduling under load uncertainty using information gap decision theory, Int. Trans. Electr. Energy Syst. 26 (2016) 464–485, https://doi.org/10.1002/ETEP.2082.